Absolute prediction of relative changes in contrast sensitivity with aberrations using a single metric of retinal image quality

Charles Leroux, Sarah Ouadi, Conor Leahy, Isabelle Marc, Christophe Fontvieille, Fabrice Bardin

Research Article | Vol. 14, No. 7 / 1 Jul 2023 / Biomedical Optics Express 3203
Biomedical Optics EXPRESS

Absolute prediction of relative changes in contrast sensitivity with aberrations using a single metric of retinal image quality

CHARLES LEROUX,[1,*] SARAH OUADI,[1] CONOR LEAHY,[2] ISABELLE MARC,[3] CHRISTOPHE FONTVIEILLE,[1] AND FABRICE BARDIN[1]

[1]Laboratoire MIPA, Université de Nîmes, Sites des Carmes, Nîmes, 30000, France
[2]Carl Zeiss Meditec, Inc., 5300 Central Parkway, Dublin, CA 94568, USA
[3]Euromov Digital Health in Motion, Univ Montpellier, IMT Mines Ales, Alès, France
*charles.leroux@unimes.fr

Abstract: Metrics of retinal image quality predict optimal refractive corrections and correlate with visual performance. To date, they do not predict absolutely the relative change in visual performance when aberrations change and therefore need to be a-posteriori rescaled to match relative measurements. Here we demonstrate that a recently proposed metric can be used to predict, in an absolute manner, changes in contrast sensitivity measurements with Sloan letters when aberrations change. Typical aberrations of young and healthy eyes (for a 6 mm pupil diameter) were numerically introduced, and we measured the resulting loss in contrast sensitivity of subjects looking through a 2 mm diameter pupil. Our results suggest that the metric can be used to corroborate measurements of visual performance in clinical practice, thereby potentially improving patient follow-ups.

1. Introduction

The effect of ocular aberrations on contrast sensitivity measurements has been investigated in a variety of experiments, involving adaptive optics visual simulators [1–9], defocusing lenses [10–12], or the subject's natural aberrations [13]. Measurements of contrast sensitivity with a sinusoidal grating are directly modeled as the product of the Modulation Transfer Function (MTF) times the Neural Transfer Function (NTF), while contrast sensitivity with letters requires more complex modeling of spatial vision to account for the extended spectra of letters.

Metrics of retinal image quality were introduced to model visual performance with letters. Metrics are direct formulas that use the optical and neuronal transfer functions of the eye. They correlate well with ratios of acuity measurements (with/without aberrations) [14–23], but only predict these ratios to within a scaling factor. The lack of absolute prediction with metrics does not prevent them from being powerful tools that predict, with through-focus calculations, the refractive correction that actually maximizes visual performance [24–28]. Depth of focus can also be predicted with through-focus calculation of a metric of retinal image quality [5,8,29–32],

Here, we seek to demonstrate a metric that potentially can predict in an absolute manner changes in visual performance with optical aberrations. When the same subject performs the visual test twice, with two different sets of optical aberrations, the effect of his/her unknown neural performance (sensitivity and noise) is mostly canceled out when computing the ratio of visual performance. With this hypothesis, Dalimier and Dainty proposed a rigorous model based on statistical decision theory that accurately predicts change in contrast sensitivity with ocular aberrations [33]. Such an absolute prediction of relative measurements is clinically relevant for following patients with ocular aberrations that are possibly changing over time. Compared to Monte-Carlo approaches that model all stages of visual performance measurements, the Dalimier and Dainty model is more direct to implement. It still requires simulation of a set of retinal

#487217 https://doi.org/10.1364/BOE.487217
Journal © 2023 Received 6 Feb 2023; revised 9 May 2023; accepted 10 May 2023; published 12 Jun 2023

Biomedical Optics EXPRESS

images that correspond to the exact set of optotypes used during the test of visual performance. To simplify the direct implementation of the Dalimier and Dainty model in clinical practice, we defined a novel metric of retinal image quality that approximates this model, and we predicted normalized measurements of contrast sensitivity in the special case of defocus, for Sloan letters of different sizes [34]. In this work, we investigate whether the same metric can also predict ratios of contrast sensitivity measurements in the presence of higher-order aberrations. Two questions arise in this investigation. We first validate, before experiments, that the metric accurately approximates the Dalimier and Dainty model for typical higher-order aberrations of healthy eyes. We then perform measurements of contrast sensitivity changes with aberrations, and compare our metric and the Dalimier and Dainty model to measurements.

2. Methods

2.1. Experiments

Four informed subjects (26-46 years of age) participated in monocular contrast sensitivity measurements, with their dominant eye and current refractive correction. We used a chin and head rest for subject stabilization and comfort. Prior informed consent was obtained from the subjects. This study conforms with the tenets of the Declaration of Helsinki.

We measured contrast sensitivity with the standard set of 10 dark Sloan letters [35,36] of 2 arcminutes gap, which corresponded to 20/40 visual acuity, on a green background. We introduced ocular aberrations numerically by convolving Sloan letters with aberrated point spread functions [37,38], generated with the statistical model of Thibos for a 6 mm pupil diameter [39]. The model fits the Indiana Aberration Study of monochromatic aberrations in a population of young eyes, subjectively refracted under cycloplegia [40]. We also measured the contrast sensitivity for Sloan letters convolved with the diffraction-limited point spread function, for a 6 mm pupil diameter. We reported ratios η of contrast sensitivity measurements:

$$\eta = \frac{CS_B}{CS_0} \tag{1}$$

where the B index stands for the blurred condition with aberrations and the 0 index stands for the aberration-free condition. Subjects viewed visual stimuli with 2 mm pupil diameter to limit the effect of their own aberrations. During each measurement session, five contrast sensitivity measurements were performed (four with aberrations, and one diffraction-limited reference). The five measurements were performed in parallel, in randomized order, to limit the effect of neural adaptation to aberrations [41–45]. Contrast sensitivity was measured with an eight-alternative choice protocol using the method of constant stimuli with randomized appearance of stimulus contrast. The subject had to choose one of eight blur-free choice letters, after the (possibly blurred) test letter was displayed for 1.5 seconds at the center of the 1.0 degree visual field. The eight choice letters were randomly selected by a computer program from the standard set of 10 Sloan letters, and were displayed after the test letter disappeared, around the center of the 1.0 degree visual field. The choice letters were of the same size and of the same font as the test letters, and were displayed by the system with a fixed 30.0% contrast. Figure 2 of Ref. [34] illustrates this display system. For each contrast sensitivity measurement, we have used 30 trials with predefined contrast values of test letters in the 1.2% – 30.0% range for aberrated letters, and in the 0.12% – 11.8% range for unaberrated letters. Each measurement session consisted of 150 trials. Contrast sensitivity was estimated as the inverse of contrast threshold for which the probability of correct response is 0.5. The measured psychometric function was fit with the cumulative normal function [46]. Measurements with fewer than 4 correct responses out of the 30 trials were discarded because they did not provide a reliable estimate of contrast sensitivity. Each of the four subjects performed five measurement sessions, during which four aberrations of the Thibos model were introduced. A total of 80 different aberrations were analyzed in this study.

Biomedical Optics EXPRESS

2.2. Models of contrast sensitivity

The informed subjects wore their current refractive correction, so we assumed that their eyes were diffraction-limited for a 2 mm pupil diameter [40,47]. We modeled visual performance with an overall Optical Transfer Function (OTF). We computed the overall OTF as the product of a numerical OTF (OTF_{num}), which numerically blurred the displayed Sloan letters, times an optical OTF (OTF_{opt}) that modeled the process of viewing the Sloan letter with a diffraction-limited eye of pupil diameter 2 mm. We noted OTF_B and OTF_0, this product in the aberrated and unaberrated condition, respectively. The corresponding MTFs, MTF_B and MTF_0, were defined as the modulus of OTF_B and OTF_0, respectively. We computed metrics of retinal image quality using a generic model of NTF. We have used the code given by Hastings et al. [48] to compute NTF for the mean age of subjects (34 years) and the retinal illuminance of our experiment (261 trolands). Figure 1(a) shows the horizontal profiles of MTF_B (dashed red line, averaged across the 80 tested aberrations), MTF_0 (dashed black line), and NTF (solid yellow line). The profiles of $MTF_B \times NTF$ and $MTF_0 \times NTF$ are shown as a solid red line and a solid black line respectively.

We defined the M metric as [34]:

$$M = \sqrt{\frac{\iint \left(NTF(f_x,f_y)MTF_B(f_x,f_y)\right)^2 df_x df_y}{\iint \left(NTF(f_x,f_y)MTF_0(f_x,f_y)\right)^2 df_x df_y}} \tag{2}$$

The M metric was defined from the Dalimier and Dainty model, which predicts η as a ratio R of "data separability". The model is computed for each set of aberrations using the simulated retinal image of the k^{th} Sloan letter ($k = 1$ to 10, as we used the 10 letters of the chart) with and without aberrations ($I_{B,k}(x,y)$ and $I_{0,k}(x,y)$ respectively):

$$R = \sqrt{\frac{\sum_{k=1}^{10} \iint [I_{B,k}(x,y) - \bar{I}_B(x,y)]^2 dxdy}{\sum_{k=1}^{10} \iint [I_{0,k}(x,y) - \bar{I}_0(x,y)]^2 dxdy}} \tag{3}$$

$\bar{I}_B(x,y)$ and $\bar{I}_0(x,y)$ were the corresponding averages (over k) of retinal images with and without aberrations, respectively. R quantifies the variability (over k) of retinal images for a fixed stimulus contrast. Because of blur, R reduces with increasing optical aberrations. The R model is not strictly speaking a metric of retinal image quality (as defined by the vision science community [25]) because it is computed for a given set of visual stimuli, in this case the 10 Sloan letters of $a = 2$ arcminutes gap. In our previous work [34], we introduced the Fourier transform of the difference between the letter O_k and the average letter $\overline{O}$ (across the $k = 1$ to 10 letters): $\tilde{\Delta}_k(f_x,f_y) = \mathcal{F}\left\{O_k(x,y) - \overline{O}(x,y)\right\}$ and re-wrote R as:

$$R = \sqrt{\frac{\sum_{k=1}^{10} \iint \left(NTF(f_x,f_y)MTF_B(f_x,f_y)\right)^2 \left|\tilde{\Delta}_k(f_x,f_y)\right|^2 df_x df_y}{\sum_{k=1}^{10} \iint \left(NTF(f_x,f_y)MTF_0(f_x,f_y)\right)^2 \left|\tilde{\Delta}_k(f_x,f_y)\right|^2 df_x df_y}} \tag{4}$$

In the limit of small Sloan letters $\tilde{\Delta}_k(f_x,f_y)$ becomes a constant function that extends over the full $\mathbb{R}^2$ domain of spatial frequency:

$$\lim_{a \to 0} \tilde{\Delta}_k(f_x,f_y) = \tilde{\Delta}_k \tag{5}$$

Biomedical Optics EXPRESS

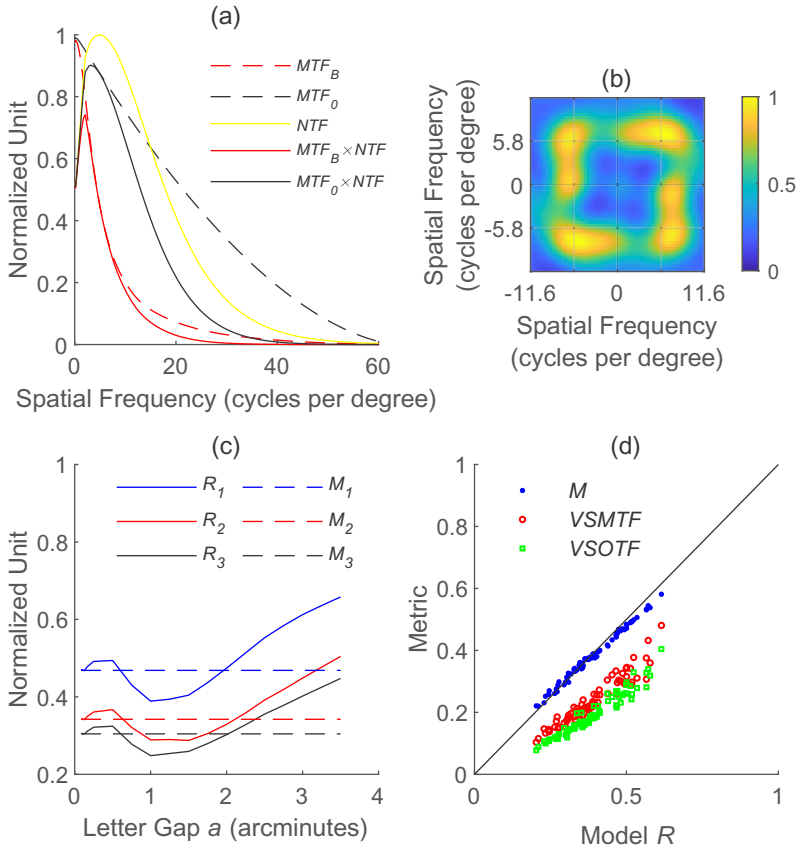

Fig. 1. (a) Horizontal profiles of the Modulation Transfer Functions: with aberration (MTF_B, average of 80 aberrations: dashed red line), without aberration (MTF_0, dashed black line), and the *NTF* model of neural transfer function (solid yellow line). The profiles of $MTF_B \times NTF$ and $MTF_0 \times NTF$ are shown as a solid red line and a solid black line respectively. (b) Letter-averaged spectrum of Sloan letters, $\sum_{k=1}^{k=10} |\tilde{\Delta}_k(f_x,f_y)|^2$. The spectrum is displayed over the ± 11.6 cycles per degree range of spatial frequencies. (c) Illustration of the $\lim_{a\to 0} R(a) = M$ convergence, for three model eyes of this study. (d) Scatter graphs of the three metrics as functions of the R model, for the $a = 2$ arcminutes letter gap of this study. Blue dot: M, red circle: *VSMTF*, green square: *VSOTF*. The solid black line denotes the $y = x$ line of perfect agreement.

In this limiting case, $\tilde{\Delta}_k$ is a scalar prefactor of integrals that cancels out in Eq. (4), which allowed us to identify the M metric as the limit of the R model, as a approaches zero:

$$\lim_{a\to 0} R(a) = M \tag{6}$$

In the current study we analyzed contrast sensitivity changes with ocular aberrations for a relatively large letter gap of $a = 2$ arcminutes (20/40 visual acuity). As a result, the $\tilde{\Delta}_k(f_x,f_y)$ spectrum only extends over a limited range of spatial frequency. Figure 1(b) shows that the letter-averaged energy spectrum, $\sum_{k=1}^{k=10} |\tilde{\Delta}_k(f_x,f_y)|^2$, is mostly band-limited in the (5-11) cycles per degree range. Despite the slow convergence of the limit in Eq. (5), the metric M reasonably approximated the $R(a)$ model for $a = 2$ arcminutes, as we show in Fig. 1(c) for three randomly selected sets of aberrations used in this study (R_1, R_2, R_3). The limit in Eq. (6) converges in similar manner for all three sets. $R(a)$ oscillates around the M value when a decreases, and the

Biomedical Optics EXPRESS

oscillation becomes smaller as $a \to 0$. At the fixed $a = 2$ arcminutes letter gap of this study, the comparison of M and R for the 80 tested aberration sets is shown as a scatter graph in Fig. 1(d), which shows the metric M (blue dots) as a function of the R model. It is close to the $y = x$ perfect agreement line (solid black line). The linear fit (not shown) is $M = 0.87R + 0.05$ ($r^2 = 0.99$). For comparison with M, we also used two other metrics of retinal image quality. The Visual Strehl ratio computed with OTF (VSOTF) metric is used in many studies because it correlates well with visual acuity [15]. We have used the *augmented* definition of VSOTF [49]:

$$VSOTF = \frac{\iint NTF(f_x,f_y)|\mathrm{Re}\{OTF_B(f_x,f_y)\}|df_x df_y}{\iint NTF(f_x,f_y)OTF_0(f_x,f_y)df_x df_y} \tag{7}$$

We also computed the VSMTF metric (Visual Strehl computed with MTF) [15], which is closely related to M as it is also defined as a norm of the $MTF \times NTF$ product :

$$VSMTF = \frac{\iint NTF(f_x,f_y)MTF_B(f_x,f_y)df_x df_y}{\iint NTF(f_x,f_y)MTF_0(f_x,f_y)df_x df_y} \tag{8}$$

In Fig. 1(d), the *VSMTF* and the *VSOTF* metrics (red circles and green squares respectively) are shown as functions of the R model. The corresponding linear fits were $VSMTF = 0.73R - 0.05$ ($r^2 = 0.90$) and $VSOTF = 0.67R - 0.06$ ($r^2 = 0.92$). In comparison with R, both *VSMTF* and *VSOTF* overestimate the contrast sensitivity loss in the presence of aberrations. The three metrics are correlated with the R model.

2.3. Comparing models to measurements

The data collected with the four subjects were pooled together. For each metric of retinal image quality and for the Dalimier and Dainty model, we analyzed the (η, model) scatter graph. The overall accuracy of each model was investigated by comparing the linear fit to the $y = x$ line using the 95 % confidence band of each fit. The agreement of each model with η measurements was also investigated using the coefficient of determination of the linear fit.

3. Results

Figure 2 shows the (η, model) scatter graphs for the R model (Fig. 2(a)) and for the three metrics of retinal image quality (Fig. 2(b): M metric, Fig. 2(c): *VSMTF* metric, Fig. 2(d): *VSOTF* metric). The solid red line of each graph shows the linear fit, and the dashed red lines show the 95 % confidence band of the fit. The solid black line shows the perfect agreement ($y = x$) line. The $y = x$ line belongs to the confidence band of the fit functions for the R model and the M metric, which indicates that R and M are accurate predictors of η measurements for this study. The *VSMTF* and *VSOTF* metrics appear biased, as the $y = x$ line does not belong to the confidence band of their fit functions. The parameters of the linear fit are summarized in Table 1. Coefficients of determination are similar, and range from 0.53 (for the *VSOTF* metric) to 0.58 (for the R model). Six contrast sensitivity measurements were disregarded (out of 80) when the subject gave less than four correct responses (out of 30 tests).

Figure 3(a) shows the statistics of η measurements, the R model, and the three metrics of retinal image quality. We show the median (red line) inside a box that limits the first and third quartiles. The box plot shows that the η measurements, the R model, and the M metric, have comparable median values (0.35, 0.37, 0.38 respectively). The median values of the *VSMTF* and *VSOTF* metrics are lower (0.22 and 0.18 respectively), and their boxes do not overlap with the η box. The statistics of the η measurements are right-skewed, with a third quartile (0.51) further from the median (0.35) than the first quartile (0.28). A Jarque-Bera test rejects the hypothesis that η measurements follow normal statistics with unknown mean and variance ($p<0.05$). The

Biomedical Optics EXPRESS

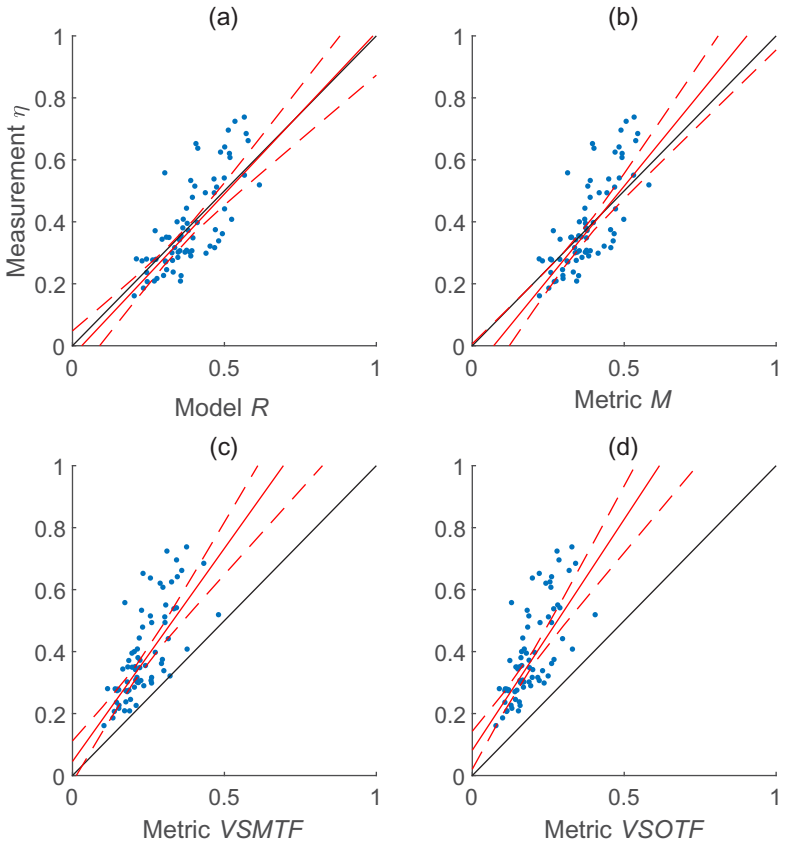

Fig. 2. Scatter graphs of (η measurement, model) pairs, for the R model (a), the M metric (b), the *VSMTF* metric (c), and the *VSOTF* metric (d). The solid red line shows the linear fit, dashed red lines delimit the 95 % confidence interval of the fit, and the solid black line shows the $y = x$ equation of perfect agreement.

Table 1. Coefficients of the $\eta = \alpha \times \text{model} + \beta$ linear fits, for the *R* model and the three metrics of retinal image quality. The linear fits are shown as red solid lines in Fig. 2(a-d)).

	slope α	intercept β	coefficient of determination r^2
R	1.04	−0.03	0.58
M	1.19	−0.08	0.57
VSMTF	1.38	0.05	0.55
VSOTF	1.49	0.08	0.53

comparison of η statistics with each model's statistics is obtained by a non-parametric, one-sample hypothesis test of the (model − η) differences. We choose the one-sample test for zero median (Wilcoxon signed rank test). The test rejects the hypothesis of zero median for the ($VSOTF - \eta$) and ($VSMTF - \eta$) differences ($p<0.001$), and does not reject this hypothesis for the ($R - \eta$) and ($M - \eta$) differences. Figures 3(b-e) show the histograms of (model-η) differences for the R model (Fig. 3(b)), and the three metrics (Fig. 3(d-e)).

Biomedical Optics EXPRESS

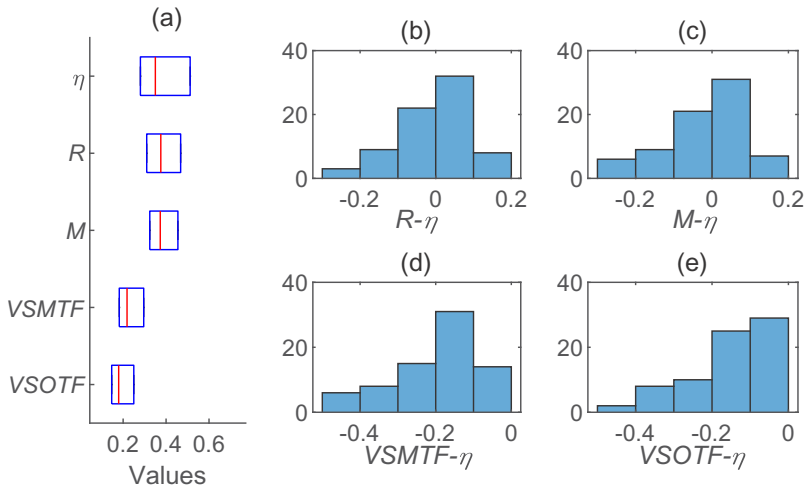

Fig. 3. (a) Median (red line), first and third quatriles (blue lines) of measurement η, model R, and metrics (M, $VSMTF$, $VSOTF$). (b-e) Histograms of (model-measurement) differences, for the R model (b), the M metric (c), the $VSMTF$ metric (d), and the $VSOTF$ metric (e).

4. Discussion

This study shows that the M metric of retinal image quality accurately predicts, overall, the ratios (with/without aberrations) of contrast sensitivity measurements with Sloan letters. Our main result to support this claim is the linear fit of the (η, M) scatter plot (Fig. 2(b)). We confirm the original finding of Dalimier and Dainty with a Landolt C test [33], as we also find that the R model is accurate (Fig. 2(a)). The M metric is an interesting trade-off between accuracy and computational simplicity, which could be directly computed in the software of a commercial aberrometer. The M metric accurately predicts the ratio of measurements and therefore approaches the predictive properties of complete models of visual performance [50–54]. On the contrary, conventional $VSOTF$ and $VSMTF$ metrics, which are phenomenological formulas to describe image quality, do not predict the actual ratios of contrast sensitivity measurements (see the linear fit of Fig. 2(c,d)). Previous studies have correlated the VSOTF and VSMTF metrics with visual acuity measurements [8,14,15,20,23,29,30], and reported high coefficients of determination of the (acuity loss, metric) linear fits. The linear fits are also potentially robust to changing experimental conditions (e.g. different pupil sizes [19]). These studies do not report on the ability of the two metrics to absolutely predict visual acuity changes with aberrations, and typically find (acuity loss, metric) linear fits with a clear departure from the $y = x$ perfect agreement. Such a linearity is however sufficient to numerically optimize the objective refraction based on aberration measurements [22–27,30,31].

We report lower coefficients of determination (see Table 1) than previous studies of the correlation between acuity loss and metrics. We emphasize that higher r^2 values may have been obtained with larger amplitudes of aberration. We have checked that the statistics of the $VSMTF$ metrics (mean logarithm value equal to −0.63 and standard deviation 0.13) match the statistics of the $VSMTF$ metric in the original paper that presented the model eyes [39]. As a comparative example, Ravikumar et al. [19] obtained r^2>0.8 for six different metrics of retinal image quality with aberrations of higher amplitudes, as they corresponded to a uniform distribution of the logarithm of $VSMTF$ in the (−1.8,−0.3) range.

Our metric, M, and the Dalimier and Dainty model, R, predict changes in contrast sensitivity with integrals of neurally-weighted modulation transfer functions and do not use phase transfer

Biomedical Optics EXPRESS

functions. This result may appear in contradiction with observations that the phase transfer function of the aberrated eye affects visual performance [55–57], and originates from the mathematical definition of the R model. Equation (3) defines the R model, which quantifies the separability of the different Sloan letters as a normalized "variance" (across the set of letters) of retinal images. The aberrated retinal images in Eq. (3) ($I_{B,k}$ for any letter k, and the average I_B) are all computed with the same optical transfer function, which we factorized to express R with the modulation (not phase) transfer function in Eq. (4). From the perspective of statistical decision theory, the R model hypothesizes that we model the subject as an ideal observer who uses a set of aberrated letters as templates, when identifying each test letter. This so-called Signal-Known-Exactly/Background-Known-Exactly (SKE/BKE) hypothesis is a basis of the Dalimier and Dainty model, from which we defined R and derived M with the small letter approximation [34]. The SKE/BKE hypothesis is also a standard approach to model subject performance during a visual test [58], as it mathematically simplifies the prediction of visual performance. Here, the use of aberrated letter templates by the ideal observer is the hypothesis behind the modulation-only dependence of R and M. It is a counter-intuitive hypothesis to model our experimental study, as the subjects experienced a priori unknown aberrations that are not their natural ones. The hypothesis that they exactly know the aberrated letters, and use perfectly matched templates, is therefore difficult to justify, but here the model gives accurate results. Our intuitive explanation for this paradox is that most aberrated letters could still be identified by subjects at high contrast. This observation would probably not hold for smaller letter sizes and/or higher aberration amplitudes, when aberrations significantly alter retinal images beyond simple contrast reduction. Consequently, we expect that the M metric is a good predictor of contrast sensitivity changes in a specific range of aberration amplitudes that also depend on the letter size. Experimental investigation of this limitation will be an important step towards the clinical applications of the M metric.

Like many authors, we took as reference the contrast sensitivity measurement without aberration. However, a potential application of the M metric could be the prediction of contrast sensitivity ratios with two sets of aberrations, when aberrations have changed over time. For some clinical cases, one may face the problem that the brain can adapt to changing aberrations [41–45]. Predictions may improve by taking account of the neural adaptation with two different neural transfer functions, corresponding to the two dates of interest, at the cost of increasing the model complexity. More generally, the influence of the neural transfer function on the model predictions was not consistently investigated in this work. Moreover, the brain constantly adapts to the visual scene [59]. Therefore, the feasibility of predicting visual performance changes over time, solely based on aberration measurements, remains an open question.

5. Conclusion

We investigated the ability of a single metric, M, to predict absolutely (with/without aberration) ratios of contrast sensitivity measurements for a set of 80 typical ocular aberrations. Predictions with the M metric appear unbiased on the (measurement,metric) scatter graphs, while conventional metrics (*VSOTF* and *VSMTF*) appear to overestimate the effect of aberrations. Coefficients of determination were similar for all metrics and may have been higher with larger aberration amplitudes. Absolute comparison of the M metric and subjective measurements of visual performance could potentially become an important part of routine patient follow-ups.

Disclosures. The authors declare no conflicts of interest.

Data Availability. Data underlying the results presented in this paper are not publicly available at this time but may be obtained from the authors upon reasonable request.

References

1. D. Williams, G.-Y. Yoon, J. Porter, A. Guirao, H. Hofer, and I. Cox, "Visual benefit of correcting higher order aberrations of the eye," J. Refractive Surg. **16**(5), S554–S559 (2000).

Biomedical Optics EXPRESS

2. G.-Y. Yoon and D. R. Williams, "Visual performance after correcting the monochromatic and chromatic aberrations of the eye," J. Opt. Soc. Am. A **19**(2), 266–275 (2002).
3. P. A. Piers, S. Manzanera, P. M. Prieto, N. Gorceix, and P. Artal, "Use of adaptive optics to determine the optimal ocular spherical aberration," J. Cataract Refractive Surg. **33**(10), 1721–1726 (2007).
4. E. Dalimier, C. Dainty, and J. L. Barbur, "Effects of higher-order aberrations on contrast acuity as a function of light level," J. Mod. Opt. **55**(4-5), 791–803 (2008).
5. H. Guo, D. A. Atchison, and B. J. Birt, "Changes in through-focus spatial visual performance with adaptive optics correction of monochromatic aberrations," Vision Res. **48**(17), 1804–1811 (2008).
6. H. Rouger, Y. Benard, and R. Legras, "Effect of monochromatic induced aberrations on visual performance measured by adaptive optics technology," J. Refractive Surg. **26**(8), 578–587 (2010).
7. P. de Gracia, S. Marcos, A. Mathur, and D. A. Atchison, "Contrast sensitivity benefit of adaptive optics correction of ocular aberrations," J. Vis. **11**(12), 5 (2011).
8. L. Zheleznyak, R. Sabesan, J.-S. Oh, S. MacRae, and G. Yoon, "Modified monovision with spherical aberration to improve presbyopic through-focus visual performance," Invest. Ophthalmol. Visual Sci. **54**(5), 3157–3165 (2013).
9. R. Sabesan, L. Zheleznyak, and G. Yoon, "Binocular visual performance and summation after correcting higher order aberrations," Biomed. Opt. Express **3**(12), 3176–3189 (2012).
10. F. Campbell and D. Green, "Optical and retinal factors affecting visual resolution," J. Physiol. **181**(3), 576–593 (1965).
11. D. A. Atchison, R. L. Woods, and A. Bradley, "Predicting the effects of optical defocus on human contrast sensitivity," J. Opt. Soc. Am. A **15**(9), 2536–2544 (1998).
12. N. C. Strang, D. A. Atchison, and R. L. Woods, "Effects of defocus and pupil size on human contrast sensitivity," Ophthalmic Physiol. Opt. **19**(5), 415–426 (1999).
13. R. Michael, O. Guevara, M. De La Paz, J. Alvarez de Toledo, and R. I. Barraquer, "Neural contrast sensitivity calculated from measured total contrast sensitivity and modulation transfer function," Acta Ophthalmol. **89**(3), 278–283 (2011).
14. X. Cheng, L. N. Thibos, and A. Bradley, "Estimating visual quality from wavefront aberration measurements," J. Refractive Surg. **19**(5), S579–S584 (2003).
15. J. D. Marsack, L. N. Thibos, and R. A. Applegate, "Metrics of optical quality derived from wave aberrations predict visual performance," J. Vis. **4**(4), 8 (2004).
16. R. A. Applegate, J. D. Marsack, and L. N. Thibos, "Metrics of retinal image quality predict visual performance in eyes with 20/17 or better visual acuity," Optometry Vis. Sci. **83**(9), 635–640 (2006).
17. E. A. Villegas, E. Alcón, and P. Artal, "Optical quality of the eye in subjects with normal and excellent visual acuity," Invest. Ophthalmol. Visual Sci. **49**(10), 4688–4696 (2008).
18. X. Cheng, A. Bradley, S. Ravikumar, and L. N. Thibos, "The visual impact of Zernike and Seidel forms of monochromatic aberrations," Optometry Vis. Sci. **87**(5), 300–312 (2010).
19. A. Ravikumar, E. J. Sarver, and R. A. Applegate, "Change in visual acuity is highly correlated with change in six image quality metrics independent of wavefront error and/or pupil diameter," J. Vis. **12**(10), 11 (2012).
20. A. Ravikumar, J. D. Marsack, H. E. Bedell, Y. Shi, and R. A. Applegate, "Change in visual acuity is well correlated with change in image-quality metrics for both normal and keratoconic wavefront errors," J. Vis. **13**(13), 28 (2013).
21. M. J. Collins, T. Buehren, and D. R. Iskander, "Retinal image quality, reading and myopia," Vision Res. **46**(1-2), 196–215 (2006).
22. L. Chen, B. Singer, A. Guirao, J. Porter, and D. R. Williams, "Image metrics for predicting subjective image quality," Optometry Vis. Sci. **82**(5), 358–369 (2005).
23. J. Bühren, K. Pesudovs, T. Martin, A. Strenger, G. Yoon, and T. Kohnen, "Comparison of optical quality metrics to predict subjective quality of vision after laser in situ keratomileusis," J. Cataract Refractive Surg. **35**(5), 846–855 (2009).
24. A. Guirao and D. R. Williams, "A method to predict refractive errors from wave aberration data," Optometry Vis. Sci. **80**(1), 36–42 (2003).
25. L. N. Thibos, X. Hong, A. Bradley, and R. A. Applegate, "Accuracy and precision of objective refraction from wavefront aberrations," J. Vis. **4**(4), 9 (2004).
26. J. Martin, B. Vasudevan, N. Himebaugh, A. Bradley, and L. Thibos, "Unbiased estimation of refractive state of aberrated eyes," Vision Res. **51**(17), 1932–1940 (2011).
27. G. D. Hastings, J. D. Marsack, L. C. Nguyen, H. Cheng, and R. A. Applegate, "Is an objective refraction optimised using the visual strehl ratio better than a subjective refraction?" Ophthalmic Physiol. Opt. **37**(3), 317–325 (2017).
28. G. D. Hastings, J. D. Marsack, L. N. Thibos, and R. A. Applegate, "Normative best-corrected values of the visual image quality metric vsx as a function of age and pupil size," J. Opt. Soc. Am. A **35**(5), 732–739 (2018).
29. L. Zheleznyak, H. Jung, and G. Yoon, "Impact of pupil transmission apodization on presbyopic through-focus visual performance with spherical aberration," Invest. Ophthalmol. Visual Sci. **55**(1), 70–77 (2014).
30. X. Cheng, A. Bradley, and L. N. Thibos, "Predicting subjective judgment of best focus with objective image quality metrics," J. Vis. **4**(4), 7 (2004).
31. M. Kilintari, A. Pallikaris, N. Tsiklis, and H. S. Ginis, "Evaluation of image quality metrics for the prediction of subjective best focus," Optometry Vis. Sci. **87**(3), 183–189 (2010).

Biomedical Optics EXPRESS

32. F. Yi, D. R. Iskander, and M. Collins, "Depth of focus and visual acuity with primary and secondary spherical aberration," Vision Res. **51**(14), 1648–1658 (2011).
33. E. Dalimier and C. Dainty, "Use of a customized vision model to analyze the effects of higher-order ocular aberrations and neural filtering on contrast threshold performance," J. Opt. Soc. Am. A **25**(8), 2078–2087 (2008).
34. C. Leroux, C. Fontvieille, C. Leahy, I. Marc, and F. Bardin, "Predicting the effects of defocus blur on contrast sensitivity with a model-based metric of retinal image quality," J. Opt. Soc. Am. A **39**(10), 1866–1873 (2022).
35. D. Pelli, J. Robson, and A. Wilkins, "The design of a new letter chart for measuring contrast sensitivity," Clinical Vis. Sci. **2**, 187–199 (1988).
36. F. Ricci, C. Cedrone, and L. Cerulli, "Standardized measurement of visual acuity," Ophthalmic Epidemiol. **5**(1), 41–53 (1998).
37. G. Burton and N. Haig, "Effects of the seidel aberrations on visual target discrimination," J. Opt. Soc. Am. A **1**(4), 373–385 (1984).
38. R. A. Applegate, J. D. Marsack, R. Ramos, and E. J. Sarver, "Interaction between aberrations to improve or reduce visual performance," J. Cataract Refractive Surg. **29**(8), 1487–1495 (2003).
39. L. N. Thibos, "Retinal image quality for virtual eyes generated by a statistical model of ocular wavefront aberrations," Ophthalmic Physiol. Opt. **29**(3), 288–291 (2009).
40. L. N. Thibos, X. Hong, A. Bradley, and X. Cheng, "Statistical variation of aberration structure and image quality in a normal population of healthy eyes," J. Opt. Soc. Am. A **19**(12), 2329–2348 (2002).
41. P. Artal, L. Chen, E. J. Fernández, B. Singer, S. Manzanera, and D. R. Williams, "Neural compensation for the eye's optical aberrations," J. Vis. **4**(4), 4 (2004).
42. L. Sawides, S. Marcos, S. Ravikumar, L. Thibos, A. Bradley, and M. Webster, "Adaptation to astigmatic blur," J. Vis. **10**(12), 22 (2010).
43. P. de Gracia, C. Dorronsoro, G. Marin, M. Hernandez, and S. Marcos, "Visual acuity under combined astigmatism and coma: optical and neural adaptation effects," J. Vis. **11**(2), 5 (2011).
44. A. Ohlendorf, J. Tabernero, and F. Schaeffel, "Neuronal adaptation to simulated and optically-induced astigmatic defocus," Vision Res. **51**(6), 529–534 (2011).
45. L. Sawides, P. de Gracia, C. Dorronsoro, M. Webster, and S. Marcos, "Adapting to blur produced by ocular high-order aberrations," J. Vis. **11**(7), 21 (2011).
46. S. A. Klein, "Measuring, estimating, and understanding the psychometric function: A commentary," Perception Psychophysics **63**(8), 1421–1455 (2001).
47. J. F. Castejón-Mochón, N. López-Gil, A. Benito, and P. Artal, "Ocular wave-front aberration statistics in a normal young population," Vision Res. **42**(13), 1611–1617 (2002).
48. G. D. Hastings, J. D. Marsack, L. N. Thibos, and R. A. Applegate, "Combining optical and neural components in physiological visual image quality metrics as functions of luminance and age," J. Vis. **20**(7), 20 (2020).
49. D. R. Iskander, "Computational aspects of the visual Strehl ratio," Optometry Vis. Sci. **83**(1), 57–59 (2006).
50. O. Nestares, R. Navarro, and B. Antona, "Bayesian model of Snellen visual acuity," J. Opt. Soc. Am. A **20**(7), 1371–1381 (2003).
51. E. Dalimier, E. Pailos, R. Rivera, and R. Navarro, "Experimental validation of a bayesian model of visual acuity," J. Vis. **9**(7), 12 (2009).
52. A. B. Watson and A. J. Ahumada, "A standard model for foveal detection of spatial contrast," J. Vis. **5**(9), 6 (2005).
53. A. B. Watson and A. J. Ahumada, "Predicting visual acuity from wavefront aberrations," J. Vis. **8**(4), 17 (2008).
54. A. B. Watson and A. J. Ahumada, "Letter identification and the neural image classifier," J. Vis. **15**(2), 15 (2015).
55. L. N. Piotrowski and F. W. Campbell, "A demonstration of the visual importance and flexibility of spatial-frequency amplitude and phase," Perception **11**(3), 337–346 (1982).
56. E. J. Sarver and R. A. Applegate, "The importance of the phase transfer function to visual function and visual quality metrics," J. Refractive Surg. **20**(5), 504–507 (2004).
57. S. Ravikumar, A. Bradley, and L. Thibos, "Phase changes induced by optical aberrations degrade letter and face acuity," J. Vis. **10**(14), 18 (2010).
58. H. H. Barrett and K. J. Myers, *Foundations of Image Science* (Wiley, 2003), Chap. **13**, pp. 801–856.
59. N. J. Majaj, D. G. Pelli, P. Kurshan, and M. Palomares, "The role of spatial frequency channels in letter identification," Vision Res. **42**(9), 1165–1184 (2002).